

## Unified Scaling Law for Earthquakes

Per Bak,<sup>1,\*</sup> Kim Christensen,<sup>2,†</sup> Leon Danon,<sup>2</sup> and Tim Scanlon<sup>2</sup>

<sup>1</sup>*Department of Mathematics, Imperial College, Queen's Gate, London SW7 2BZ, United Kingdom*

<sup>2</sup>*Blackett Laboratory, Imperial College, Prince Consort Road, London SW7 2BW, United Kingdom*

(Received 11 August 2001; published 10 April 2002)

We show that the distribution of waiting times between earthquakes occurring in California obeys a simple unified scaling law valid from tens of seconds to tens of years. The short time clustering, commonly referred to as aftershocks, is nothing but the short time limit of the general hierarchical properties of earthquakes. There is no unique operational way of distinguishing between main shocks and aftershocks. In the unified law, the Gutenberg-Richter  $b$  value, the exponent  $-1$  of the Omori law for aftershocks, and the fractal dimension  $d_f$  of earthquakes appear as critical indices.

DOI: 10.1103/PhysRevLett.88.178501

PACS numbers: 91.30.Dk, 05.65.+b, 89.75.Da

Earthquakes are a complicated spatiotemporal phenomenon. The number of earthquakes with a magnitude  $M > m$  is given by the Gutenberg-Richter law [1]. In addition to the regularity in the rate of occurrence, earthquakes display a complex spatiotemporal behavior [2,3]. The spatial distribution of epicenters is fractal and they occur on a fractal-like structure of faults [3,4]. Short-range temporal correlations between earthquakes are expressed by Omori's law [5], which states that immediately following a main earthquake there is a sequence of aftershocks whose frequency decays with time as  $T^{-\alpha}$ ,  $\alpha \approx 1$ . This has led to the commonly held belief that aftershocks are caused by a different relaxation mechanism than the main shocks.

The observed temporal complex behavior is obviously of dynamical origin. However, the statistics of earthquakes, as well as the geometrical fractal structure displayed by the faults and by the spatial distribution of epicenters, is also a result of a dynamical process and one might speculate whether it is possible to unify these observations.

We propose a unified scaling law for the waiting times between earthquakes, expressing a hierarchical organization in time, space, and magnitude. There is a correlated regime where the distribution of waiting times between earthquakes is a power law  $T^{-\alpha}$ ,  $\alpha \approx 1$  and an uncorrelated regime. However, the waiting time interval for the crossover between the two regimes for earthquakes larger than a given magnitude depends on the area and magnitude under consideration.

An earthquake catalog covering the period 1984–2000 in a region of California spanning  $20^\circ\text{N}$ – $45^\circ\text{N}$  latitude and  $100^\circ\text{W}$ – $125^\circ\text{W}$  longitude was analyzed [6]. The total number of recorded earthquakes in the catalog is 335 076. The number of earthquakes  $N(M > m)$  with a magnitude larger than  $m$  is given by the Gutenberg-Richter law [1]  $\log_{10} N(M > m) \propto -bm$ ,  $b \approx 0.95$  (see Fig. 1).

The spatiotemporal analysis was carried out as follows. We covered the region with a grid with cells of size  $L \times L$  (see Fig. 2) and defined the waiting time  $T$  as the time interval between the beginning of two successive earth-

quakes. We then measured  $P_{S,L}(T)$ , the distribution of waiting times  $T$ , between earthquakes occurring within range  $L$  whose magnitudes are greater than  $m = \log(S)$ .

Figure 3 shows the resulting set of curves  $P_{S,L}(T)$ , for time scales ranging from seconds to 16 years, for several values of  $S$  and  $L$ , plotted on double logarithmic scale. Obviously, the curves differ widely. Some general trends can be seen, however. There is a linear regime, indicating a power-law distribution, extending up to a cutoff indicating an upper limit of the waiting time. For fixed cell size  $L$  and increasing cutoff  $S$  (or  $m$ ), the range of the power-law regime increases. For fixed cutoff  $S$  and increasing cell size  $L$ , the range of the power-law regime decreases [7].

In Fig. 4, the curves are replotted in terms of rescaled coordinates. The  $x$  axis is chosen as  $x = TS^{-b}L^{d_f}$ , and the  $y$  axis represents  $y = T^\alpha P_{S,L}(T)$ . The rescaling causes a

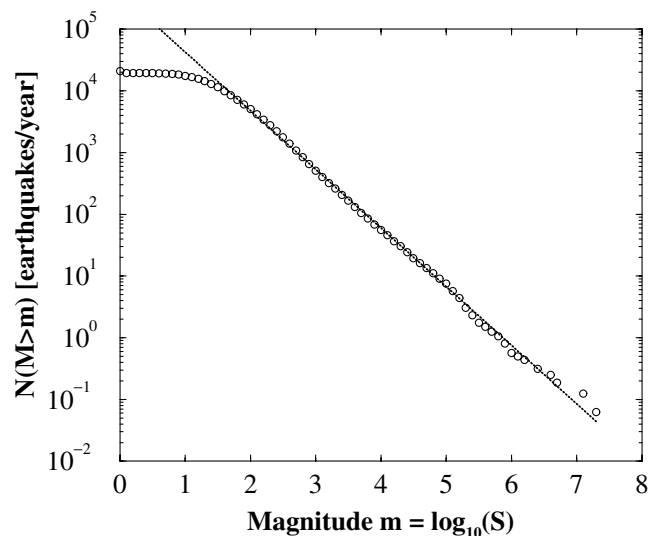


FIG. 1. The number of earthquakes  $N(M > m)$  with a magnitude larger than  $m$  per year (open circles). The dashed line is the Gutenberg-Richter law  $\log_{10} N(M > m) \propto -bm$ ,  $b = 0.95$ . The deficit at small magnitude  $m \leq 2$  is related to the problems with detecting small earthquakes, so only earthquakes with  $m \geq 2$  will be considered.

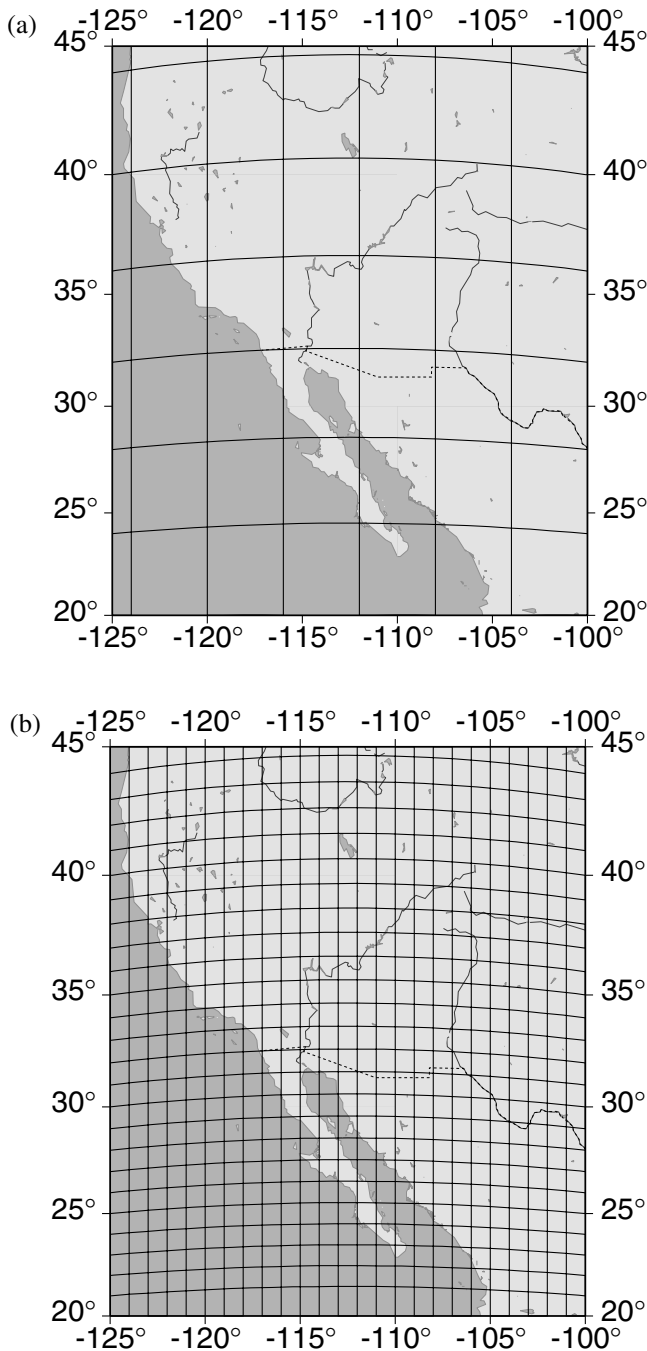


FIG. 2. The region of California divided into grids of two different cell sizes (a)  $L = 4^\circ$  and (b)  $L = 1^\circ$ .

shift of the curves in Fig. 3 that depends on  $L$  and  $S$ . For a suitable choice of the interval exponent  $\alpha$ , the magnitude exponent  $b$ , and the spatial dimension  $d_f$ , all the data collapse nicely onto a single well-defined curve  $f(x)$ , that is,

$$T^\alpha P_{S,L}(T) = f(TS^{-b}L^{d_f}). \quad (1)$$

This equation expresses the unified scaling law for earthquakes. The function  $f(x)$  consists of a constant part and a decaying part, separated by a sharp kink. The constant

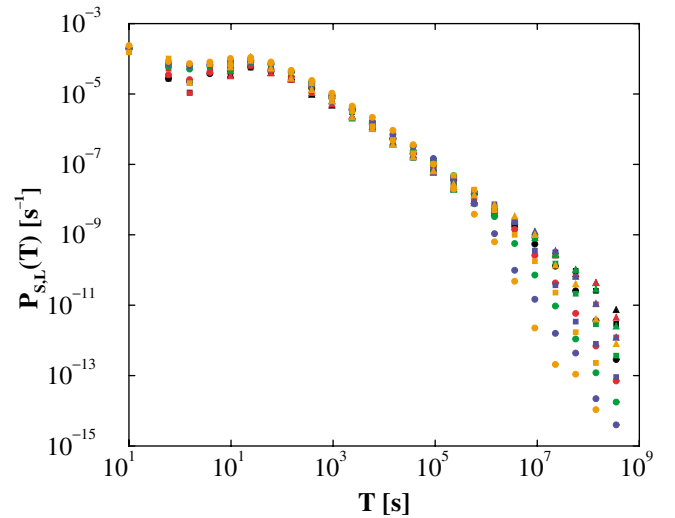


FIG. 3 (color). The distribution  $P_{S,L}(T)$  of interoccurrence time  $T$  between earthquakes with magnitude  $m$  greater than  $\log_{10}(S)$  within an area of linear size  $L$ . The solid circles, squares, and triangles correspond to cutoffs  $m = \log_{10}(S) = 2, 3, \text{ and } 4$ , respectively. The color coding represents the linear size  $L = 0.25^\circ$  (black),  $0.5^\circ$  (red),  $1^\circ$  (green),  $2^\circ$  (blue), and  $4^\circ$  (orange) of the cells covering California. For  $T < 40$  s, earthquakes overlap and individual earthquakes cannot be resolved. This causes the deficit for small  $T$ , so only intervals  $T > 38$  s will be considered in the following. Notice that, for fixed cutoff magnitude  $m$  but decreasing linear size  $L$ , the deviation from the Omori law  $T^{-\alpha}$ ,  $\alpha \approx 1$  sets in for larger values of  $T$ . On the contrary, with fixed linear size  $L$  but decreasing cutoff magnitude  $m$ , the deviation from the Omori law  $T^{-\alpha}$ ,  $\alpha \approx 1$  sets in for smaller values of  $T$ .

part corresponds to the linear, power-law part in Fig. 3 since we have multiplied  $P_{S,L}(T)$  with  $T^\alpha$ . Any deviation from power-law behavior would show up dramatically in this type of plot. *Nevertheless, the function is approximately constant over 8 orders of magnitude.* The rapidly decaying part is consistent with an exponential decaying function implying an uncorrelated regime for large values of  $x$ . This is indeed what one would expect on physical grounds: earthquakes that are separated by large enough distances or long waiting times will be uncorrelated.

The index  $\alpha \approx 1$  can be identified as the Omori-law exponent for aftershocks,  $b \approx 1$  is the  $b$  value in the Gutenberg-Richter law, and  $d_f \approx 1.2$  describes the  $2d$  fractal dimension of the location of epicenters projected onto the surface of the Earth.

The data collapse implies that the waiting time distribution depends on  $T$ ,  $S$ , and  $L$  only through the variable  $x$ . Only critical processes exhibit this type of data collapse, known as scaling in critical phenomena [8], so our analysis demonstrates that earthquakes are a self-organized critical (SOC) phenomenon [9–11], as had been anticipated from the existence of the Gutenberg-Richter law [12–15]. The data collapse shows that there is no separate relaxation mechanism for aftershocks. The three exponents  $\alpha$ ,  $b$ , and  $d_f$  characterizing earthquakes emerge as critical indices in

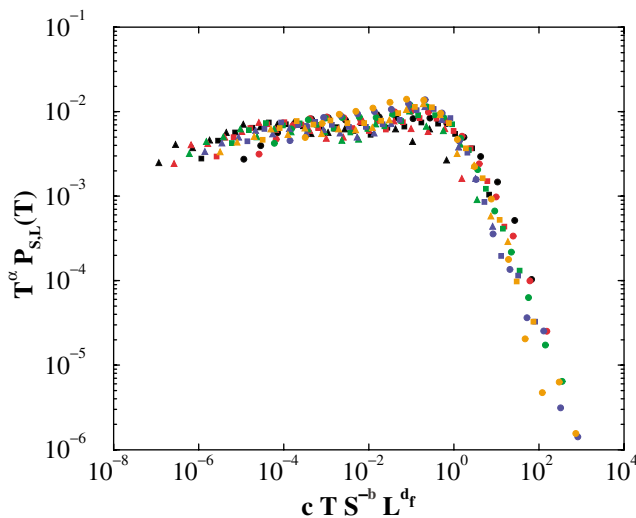


FIG. 4 (color). The data in Fig. 3 with  $T > 38$  s replotted with  $T^\alpha P_{S,L}(T)$  as a function of the variable  $x = cTS^{-b}L^{d_f}$ ,  $c = 10^{-4}$ . The data collapse implies a unified law for earthquakes. The Omori law exponent  $\alpha = 1$ , Gutenberg-Richter value  $b = 1$ , and fractal dimension  $d_f = 1.2$  have been used in order to collapse all the data onto a single, unique curve  $f(x)$ . The estimated uncertainty in the exponents is less than 0.2. The function  $f$  is constant for  $x < 1$ , corresponding to the correlated Omori law regime, while it is decaying fast for large arguments  $x > 1$ , associated with the uncorrelated regime of earthquakes. Whether two earthquakes are to be categorized as belonging to a correlated or uncorrelated sequence does not depend independently on the values of  $T$ ,  $S$ , and  $L$  but only on the value of the product  $x = TS^{-b}L^{d_f}$ .

the unified law. The estimated uncertainty in the values of the critical indices is less than 0.2. Whether the critical exponents vary with region and maybe even with time is an interesting question that is outside the scope of this Letter but we urge further studies in that direction.

Depending on the value of scaling argument  $x$ , and thus the chosen values of  $L$  and  $m$  (or  $S$ ), two successive earthquakes will either be correlated, for  $x$  small (i.e., to the left of the kink in Fig. 4), or uncorrelated, for  $x$  large (i.e., to the right of the kink in Fig. 4).

Depending on the length scale  $L$  of observations, and the magnitude  $m$  (or  $S$ ) chosen, the correlated Omori  $T^{-\alpha}$  regime may range from seconds to tens of years (and probably much longer if data were available). If the earthquakes are correlated they may be interpreted as belonging to an aftershock sequence. If they are uncorrelated, they may be interpreted as main events. This interpretation, however, depends on  $L$  and  $m$  through the variable  $x = TS^{-b}L^{d_f}$  and has no absolute meaning. Therefore, there is no unique way of characterizing earthquakes as aftershocks or main events unless both  $L$  and  $S$  are defined.

To summarize, the short time correlations given by Omori's law is just the short time limit of a general hierarchical scaling phenomenon occurring at all accessible time scales. Amazingly, the statistics of aftershocks occurring

within minutes of an earthquake can be simply related to the statistics of earthquakes separated by tens of years.

One may think of the value of  $m$  (or  $S$ ) at the kink as being a "characteristic" magnitude of earthquakes. However, since the position of the kink is a function of  $x$ , not  $m$  (or  $S$ ), one cannot specify the magnitude of the characteristic earthquake without at the same time specifying a time scale and an area. However, there is no special time scale that can play any absolute role for the dynamics of earthquakes, limited at the upper end by the time scale of tectonic plate motion and at the lower end by the duration of earthquakes.

How should one physically understand the fundamental law, Eq. (1)? Let us first discuss the meaning of the scaling variable  $x = TS^{-b}L^{d_f}$ . The quantity  $S^{-b}L^{d_f}$  appearing in its definition is a measure of the average number of earthquakes per time unit with magnitude greater than  $m = \log_{10}(S)$  occurring within the range  $L$ . Thus,  $x$  is a measure of the average number of such earthquakes occurring within a time interval  $T$ . The law states that the distribution of waiting times depends only on this number. When this number exceeds a well-defined value (the position of the kink in Fig. 4), the earthquakes sharply become less correlated.

Think of earthquakes being generated by "processes," each producing a sequence of correlated earthquakes with a  $T^{-\alpha}$  distribution. These processes correspond to a sequence of avalanches in self-organized critical models of complex phenomena. Visually, one might think of the processes as the activity associated with dynamically changing fault segment patterns. The law indicates that the crust operates in the true SOC slow-driving regime [16], where the individual processes (avalanches) do not overlap. Because of the nonzero driving rate, several spatially separated processes are active simultaneously. The kink on the  $f$  curve indicates the point where one crosses into the regime where spatially independent earthquakes, belonging to different processes, are sampled within a window spanned by  $T$  and  $L$ . For small enough  $L$  and  $T$  only a single, correlated process is sampled.

We thank C. Scholz for advising us on earthquake catalogs. P.B. acknowledges helpful discussions with M. Paczuski. K.C. gratefully acknowledges the financial support of U.K. EPSRC through Grants No. GR/R44683/01 and No. GR/L95267/01.

\*Email address: bak@alf.nbi.dk

†Email address: k.christensen@ic.ac.uk

- [1] B. Gutenberg and C. F. Richter, *Bull. Seismol. Soc. Am.* **34**, 185 (1944).
- [2] Y. Y. Kagan and D. D. Jackson, *J. Geophys. Res.* **96**, 419 (1991).
- [3] D. Marsan *et al.*, *J. Geophys. Res.* **105**, B12, 28 081 (2000).
- [4] P. G. Okubo and K. J. Aki, *J. Geophys. Res.* **92**, 345 (1987).

- [5] F. Omori, J. Coll. Sci. Imper. Univ. Tokyo **7**, 111 (1895).
- [6] The Southern California Seismographic Network catalogs 1984.cat–2000.cat can be downloaded from the Southern California Earthquake Data Centre web site <http://www.scecdc.scec.org/ftp/catalogs/SCSN/>.
- [7] Davidsen and Schuster have shown the  $T^{-1}$  behavior for a single set of  $S$  and  $L$  [see J. Davidsen and H. G. Schuster, A Simple Model for  $1/f^\alpha$  Noise (to be published)].
- [8] J. M. Yeomans, *Statistical Mechanics of Phase Transitions* (Clarendon Press, Oxford, 1992).
- [9] A system displaying SOC does not necessarily imply Poissonian waiting-time statistics. For example, the Olami-Feder-Christensen spring block model of earthquakes displays a crossover from Poissonian statistics of the quiescent time when events of all sizes are considered to a power-law-type statistics when considering earthquakes greater than a certain size  $\log(S)$ ; see, e.g., Fig. 7 in K. Christensen and Z. Olami, J. Geophys. Res. **97**, 8729 (1992).
- [10] P. Bak, C. Tang, and K. Wiesenfeld, Phys. Rev. Lett. **59**, 381 (1987).
- [11] P. Bak, *How Nature Works: The Science of Self-Organised Criticality* (Copernicus, New York, 1996); *ibid.* (Copernicus, Oxford, 1997).
- [12] A. Sornette and D. Sornette, Europhys. Lett. **9**, 197 (1989).
- [13] K. Ito and M. Matsuzaki, J. Geophys. Res. **95**, 6853 (1990).
- [14] P. Bak and C. Tang, J. Geophys. Res. **94**, 15 635 (1989).
- [15] Z. Olami, H. J. S. Feder, and K. Christensen, Phys. Rev. Lett. **68**, 1244 (1992).
- [16] A. Corral and M. Paczuski, Phys. Rev. Lett. **83**, 572 (1999).